Journal of Mathematical Sciences: Advances and Applications
Volume 46, 2017, Pages 97-114
Available at http://scientificadvances.co.in
DOI: http://dx.doi.org/10.18642/jmsaa_7100121857

CAPACITY BOUND AND BER PERFORMANCE OF OFDM SYSTEM IN HIGH-MOBILITY SCENARIOS

LEI LIN

School of Mathematics and Systems Science
Guangdong Polytechnic Normal University
Guangzhou 510665
P. R. China
e-mail: linlei2@mail2.sysu.edu.cn

Abstract

In this paper, we investigate the effect of velocity and channel information on the capacity of orthogonal frequency division multiplexing (OFDM) system in very rapidly time-varying fading channels. Lower bounds on the capacity of OFDM system in fast time-varying channels with perfect and imperfect channel state information (CSI) are derived. Simulation results show two main conclusions. One is that the capacity bounds change very little with increasing velocity in the channel with perfect CSI. Another is that the transmission performance is decreased quickly by the increased channel estimation errors due to high mobilities in the channel with imperfect CSI. Furthermore, we adopt block Markov superposition transmission (BMST) code to verify the conclusions.

1. Introduction

As an efficient solution to meet the growing demand for multimedia wireless communications, orthogonal frequency division multiplexing (OFDM) has been widely adopted for broadband wireless communication

2010 Mathematics Subject Classification: 68M10, 68P30, 90B18.
Keywords and phrases: high mobility, time-varying channel, OFDM, capacity, imperfect CSI.
Received July 8, 2017

systems [1]. Actually, it has previously been seen that OFDM can significantly increase spectral efficiency and robustness against multipath distortions [2]. With the rapid development of high-speed trains in the world, OFDM has also been regarded as a promising candidate for high-mobility wireless communication. However, there are several tough problems for the application of OFDM systems in high-mobility environments, such as the penetration loss, frequent handoffs [3], severe Doppler spread and channel estimation error [4]. There have been many works devoted to solving these problems about the loss of the performance in the OFDM system, e.g., [5-7]. On the other hand, the capacity of the OFDM systems under the high-mobility environments is still unknown. Although, there exists some literatures on the capacity of high-mobility systems or OFDM systems. For example, in [8], the authors discussed the ergodic and outage capacity for Ricean fading channel with shadow fading in high-mobility environments. In [9], the statistical model of fading channels was described and the theoretical capacity expressions of time-selective channel and frequency-selective channel were obtained, respectively. In [10, 11], the capacity of OFDM-based spatial multiplexing systems and MIMO-OFDM systems with imperfect channel information were presented, respectively. Nevertheless, these articles are not for the dedicated rapidly time-varying OFDM systems with high-mobility environment, in which each subcarrier undergoes a Doppler spreading effect that destroys the subcarrier orthogonality, producing significant intercarrier interference (ICI). To the best of our knowledge, no previous work considered the capacity of the OFDM system under the high mobility environments.

In this paper, we consider OFDM system over rapidly time-varying fading channels with high-mobility environment. Firstly, we assume that the CSI is perfectly known at the receiver but unknown to the transmitter. The effect of the ICI on the capacity of the time-varying OFDM system with perfect CSI is investigated. Regarding ICI as part of noise, we derive a lower bound of capacity for the time-varying OFDM system and show the impact of the velocity on the capacity bound. Secondly, the lower bound is extended to the channel with imperfect CSI. In this case, the imperfections in CSI, due mainly to the channel

estimation errors, play a critical role in impacting the capacity bound. We present the effect of channel estimation errors on the capacity bound of the high-mobility channel. In order to verifying our results, a class of spatially coupled codes, block Markov superposition transmission (BMST) code, first proposed in [12], is adopted to the time-varying OFDM system. BER performance curves are provided to analyze whether the conclusions are valid.

The rest of this article is organized as follows. In Section 2, we introduce the system model. In Section 3, lower bounds on the capacity of OFDM system in fast time-varying channels with perfect and imperfect CSI are derived. Also simulation results are presented in this section. Section 4 introduces the encoding and decoding algorithms of BMST code. Finally, we use BMST code to verify the conclusions in Section 5.

In this paper, $E[\cdot]$ denotes the statistical expectation. The notation $|\cdot|$ indicates the number of elements, and $\|\cdot\|$ denotes the Euclidean norm. The notations $(\cdot)^T$, $(\cdot)^H$, and $(\cdot)^*$ denote transpose, Hermitian transpose, and conjugation, respectively. $\mathrm{diag}(\cdot)$ denotes a diagonal matrix with the main diagonal elements given by $(\cdot)$. The notation $\mathrm{tr}(\cdot)$ denotes the trace of the matrix given by $(\cdot)$.

$$H_t = \begin{bmatrix} h_0(0) & 0 & \cdots & 0 & 0 & \cdots & 0 \\ h_1(1) & h_0(1) & 0 & \cdots & 0 & \cdots & 0 \\ \vdots & \ddots & \ddots & \ddots & \ddots & \ddots & \vdots \\ h_{L-1}(L-1) & h_{L-2}(L-1) & \ddots & h_0(L-1) & \ddots & \ddots & 0 \\ 0 & \ddots & \ddots & \ddots & \ddots & \ddots & 0 \\ 0 & \cdots & \cdots & h_{L-1}(N-1) & h_{L-2}(N-1) & \cdots & h_0(N-1) \end{bmatrix}. \tag{1}$$

2. System Model

Consider a single-input single-output (SISO) coded OFDM system with N subcarriers over rapidly time-varying channels depicted in Figure 1. The symbol transmitted on the k-th subcarrier is denoted by x_k.

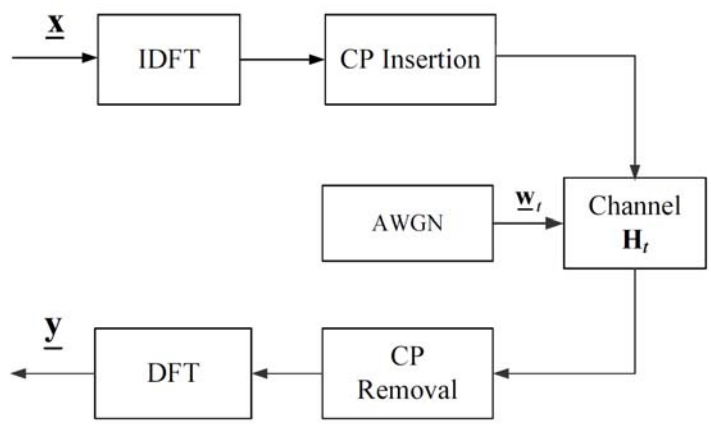

Figure 1. The block diagram of the coded OFDM system.

Defining $\mathbf{x} = [x_0, \cdots, x_{N-1}]^T$ as the vector that collects the data x_k. We assume that the average symbol energy $E_x = E[\|x_i\|^2] = 1$. The time-domain transmitted signal can be expressed as

$$s(n) = \frac{1}{\sqrt{N}} \sum_{k=0}^{N-1} x_k e^{j2\pi kn/N}, \; -L \le n \le N-1, \tag{2}$$

where L is the length of the cyclic prefix. Assuming time and frequency synchronization at the receiver side, the received signal can be written as

$$r(n) = \sum_{\ell=0}^{L-1} h_\ell(n) s(n-\ell) + w(n), \tag{3}$$

where $h_\ell(n)$ is the channel impulse response of the ℓ-th tap at time n and $w(n)$ is the complex additive white Gaussian noise (AWGN) with

zero mean and variance σ_w^2. We assume time varying multipath fast fading channel, and a Jakes' Doppler spectrum [13] with the maximum Doppler frequency $f_d = f_c v / c$, where f_c is the carrier frequency (Hz), v is the speed of the mobile terminal (km/h), and c is the speed of light. Assume that the maximum channel delay spread is less than or equal to the cyclic prefix length L. The k-th subcarrier output from the discrete Fourier transform (DFT) can be expressed as

$$y_k = \frac{1}{\sqrt{N}} \sum_{n=0}^{N-1} r_n e^{j2\pi kn/N}. \tag{4}$$

Clearly, the Equation (4) can be rewritten as [14]

$$sy_k = H_k x_k + i_k + w_k, \tag{5}$$

where

$$H_k = \frac{1}{N} \sum_{n=0}^{N-1} H_k(n); \tag{6}$$

$$i_k = \frac{1}{N} \sum_{m=0, m \neq k}^{N-1} \left[\sum_{n=0}^{N-1} H_m(n) x_m e^{j2\pi n(m-k)/N} \right]; \tag{7}$$

$$w_k = \frac{1}{\sqrt{N}} \sum_{n=0}^{N-1} w(n) e^{j2\pi k\ell/N}. \tag{8}$$

$H_k(n)$ in (6) represents the DFT of the time-varying channel impulse response at time n, defined as $H_k(n) = \sum_{\ell=0}^{L-1} h(n, \ell) e^{j2\pi k\ell/N}$ and i_k in (7) can be regarded as the ICI on the k-th subcarrier. The variance of w_k is σ_w^2. Note that $\mathbb{E}[h_\ell(n) h_{\ell+\Delta\ell}^*(n + \Delta n)] = J_0(2\pi f_d T_{ofdm} \Delta n / N)$, where T_{ofdm} is the duration of useful OFDM symbol and $J_0(\cdot)$ is the zeroth-order Bessel function of first kind. Equivalently, in a matrix form (5) can be expressed as

$$\mathbf{y} = \mathrm{diag}(\boldsymbol{H})\mathbf{x} + \mathbf{i} + \mathbf{w}, \tag{9}$$

where $\boldsymbol{H} = \boldsymbol{F}\boldsymbol{H}_t\boldsymbol{F}^H$, $\mathbf{i} = \boldsymbol{H}'\mathbf{x}$, F is the unitary DFT matrix of size N, $\boldsymbol{H}_t$ is the time domain matrix shown in Equation (1), $\boldsymbol{H}'$ is matrix $\boldsymbol{H}$ with the main diagonal elements set to zeros and $\mathbf{w} = [w_0, w_1, \cdots, w_{N-1}]^T$.

3. Capacity Bound of the Time-Varying OFDM Systems

In this section, lower capacity bounds of OFDM system under fast fading channels with perfect and imperfect CSI at the receiver are obtained.

3.1. Capacity bound of the time-varying OFDM systems with perfect CSI

We first consider the situation where the CSI is perfectly known at the receiver but unknown at the transmitter. A natural way is to regard the ICI per subcarrier as a complex Gaussian noise with zero mean and variance P_{ICI} [1]. Then the system model shown in (9) is transformed into the following time-invariant OFDM system:

$$\mathbf{y} = \mathrm{diag}(\boldsymbol{H})\mathbf{x} + \tilde{\mathbf{w}}, \tag{10}$$

where $\tilde{\mathbf{w}}$ can be treated as the noise vector whose entries are complex Gaussian variables with zero mean and variance $P_{ICI} + \sigma_w^2$. By computing the capacity of the time-invariant OFDM system, we can obtain a lower capacity bound of the time-varying OFDM system in (9). According to [10], the capacity of the channel in (10) can be taken from the following formula:

---

[1] P_{ICI} also represents the ICI power. When the number of subcarriers is large, the ICI power of the k-th subcarrier is independent of the subcarrier index k [15].

$$I(\mathbf{x};\ \mathbf{y}|\boldsymbol{H}) = \frac{1}{N} E_{\boldsymbol{H}}\left[\log_2 \det\left[\boldsymbol{I}_N + \frac{\operatorname{diag}(\boldsymbol{H})E[\mathbf{x}\mathbf{x}^H](\operatorname{diag}(\boldsymbol{H}))^H}{\sigma_w^2 + P_{ICI}}\right]\right], \quad (11)$$

where $\boldsymbol{I}_N$ is an $N \times N$ unit matrix. Note that the symbols in each subcarrier is uncorrelated, so $E[\mathbf{x}\mathbf{x}^H] = E_x \boldsymbol{I}_N = \boldsymbol{I}_N$. Thus, the lower capacity bound C_L of the time-varying OFDM system with perfect CSI can be written as

$$C_L = \frac{1}{N} E_{\boldsymbol{H}}\left[\log_2 \det\left[\boldsymbol{I}_N + \frac{\operatorname{diag}(\boldsymbol{H})(\operatorname{diag}(\boldsymbol{H}))^H}{\sigma_w^2 + P_{ICI}}\right]\right]$$

$$= \frac{1}{N} E_{\boldsymbol{H}}\left\{\sum_{k=0}^{N-1} \log_2\left[1 + \frac{\gamma H_k H_k^*}{1 + \gamma P_{ICI}}\right]\right\}, \quad (12)$$

where $\gamma = \frac{1}{\sigma_w^2}$ is the signal to noise radio (SNR). For high SNR, i.e., when $\gamma \to \infty$, it can be seen that

$$C_L^{\infty} = \frac{1}{N} E_{\boldsymbol{H}}\left\{\sum_{k=0}^{N-1} \log_2\left[1 + \frac{H_k H_k^*}{P_{ICI}}\right]\right\}. \quad (13)$$

Now we give the computing method of P_{ICI}. Obviously,

$$P_{ICI} = \frac{1}{N} E_{\mathbf{i}}[\operatorname{tr}(\mathbf{i}\mathbf{i}^H)] \overset{(a)}{=} E[\|i_k\|^2]$$

$$= \sum_{m=0,\, m\neq k}^{N-1} E_x \cdot \frac{1}{N^2}\left(N + 2\sum_{n=1}^{N-1}(N-n) J_0 R_h(nT_{ofdm}) \times \cos\left(\frac{2\pi n(m-k)}{N}\right)\right)$$

$$\overset{(b)}{=} 1 - \frac{1}{N^2}\left(N + 2\sum_{n=1}^{N-1}(N-n) J_0 R_h(nT_{ofdm})\right), \quad (14)$$

where (a) is due to the law of large numbers and (b) holds because $\sum_{m=0}^{N-1} \cos\left(\frac{2\pi n(m-k)}{N}\right) = 0$ and $E_x = 1$.

3.2. Capacity bound of the time-varying OFDM systems with imperfect CSI

In most of practical systems, it is difficult to obtain perfect CSI at the transmitter. Adopting minimum mean square error (MMSE) estimation, we assume that the estimation of channel gains is $\hat{\boldsymbol{H}} = \boldsymbol{H} + \varepsilon$, in which ε denotes the channel estimation error matrix whose entries is distributed according to $\mathcal{CN}(0, \sigma_\varepsilon^2)$ and is independent of channel gains $\boldsymbol{H}$. In this case, the system can be regarded as

$$\mathbf{y} = (\hat{\boldsymbol{H}} - \varepsilon)\mathbf{x} + \mathbf{w}. \tag{15}$$

We can also rewrite (15) into the following equation:

$$\mathbf{y} = \mathrm{diag}(\hat{\boldsymbol{H}})\mathbf{x} + \hat{\mathbf{i}} + \mathbf{w}, \tag{16}$$

where $\hat{\mathbf{i}} = (\hat{\boldsymbol{H}}' - \varepsilon)\mathbf{x}$ and $\hat{\boldsymbol{H}}'$ is matrix $\hat{\boldsymbol{H}}$ with the main diagonal elements set to zeros. Similarly, we can assume that $\hat{\mathbf{i}}$ is a complex Gaussian vector whose entries is distributed according to $\mathcal{CN}(0, \hat{P}_{ICI})$. Then, (16) can be expressed as

$$\mathbf{y} = \mathrm{diag}(\hat{\boldsymbol{H}})\mathbf{x} + \hat{\mathbf{w}}, \tag{17}$$

where the entries of $\hat{\mathbf{w}}$ are complex Gaussian variables with mean zero and variance $\hat{P}_{ICI} + \sigma_\varepsilon^2$. Similar to the method used in previous subsection, we can get a lower capacity bound of the time-varying OFDM system with imperfect CSI by means of computing the capacity of the time-invariant OFDM system in (17). Therefore, a lower capacity bound $\hat{C}_L$ of the time-varying OFDM system with imperfect CSI is expressed as

$$\hat{C}_L = I(\mathbf{x}; \mathbf{y}|\hat{\boldsymbol{H}})$$

$$= \frac{1}{N} E_{\hat{\boldsymbol{H}}}\left[\log_2 \det\left[\boldsymbol{I}_N + \frac{\operatorname{diag}(\hat{\boldsymbol{H}})E[\mathbf{x}\mathbf{x}^H]\left(\operatorname{diag}(\hat{\boldsymbol{H}})\right)^H}{\sigma_w^2 + \hat{P}_{ICI}}\right]\right]$$

$$= \frac{1}{N} E_{\hat{\boldsymbol{H}}}\left[\log_2 \det\left[\boldsymbol{I}_N + \frac{\operatorname{diag}(\hat{\boldsymbol{H}})\left(\operatorname{diag}(\hat{\boldsymbol{H}})\right)^H}{\sigma_w^2 + \hat{P}_{ICI}}\right]\right]$$

$$= \frac{1}{N} E_{\hat{\boldsymbol{H}}}\left\{\sum_{k=0}^{N-1} \log_2\left[1 + \frac{\gamma \hat{H}_k \hat{H}_k^*}{1 + \gamma \hat{P}_{ICI}}\right]\right\}, \tag{18}$$

where $\hat{H}_k$ represents the k-th main diagonal element of $\hat{\boldsymbol{H}}$. The next step is to derive the value of $\hat{P}_{ICI}$.

$$\hat{P}_{ICI} = \frac{1}{N} E_{\hat{\mathbf{i}}}\left[\operatorname{tr}(\hat{\mathbf{i}}\hat{\mathbf{i}}^H)\right] = E[\|\hat{i}_k\|^2]$$

$$= E[\|i_k - \varepsilon_k x_k\|^2] \overset{(a)}{=} E[\|i_k\|^2] + E[\|\varepsilon_k x_k\|^2]$$

$$\overset{(b)}{=} E[\|i_k\|^2] + E[\|\varepsilon_k\|^2]E[\|x_k\|^2] \overset{(c)}{=} E[\|i_k\|^2] + E[\|\varepsilon_k\|^2$$

$$= P_{ICI} + \sigma_\varepsilon^2, \tag{19}$$

where $\hat{i}_k$ is the k-th element of $\hat{\mathbf{i}}$ and ε_k is the k-th main diagonal element of ε. (a) and (b) hold because i_k, ε_k, and x_k are independent. (c) is due to $E[\|x_k\|^2] = 1$. Replacing (19) into (18), we get

$$\hat{C}_L = \frac{1}{N} E_{\hat{\boldsymbol{H}}}\left\{\sum_{k=0}^{N-1} \log_2\left[1 + \frac{\gamma \hat{H}_k \hat{H}_k^*}{1 + \gamma(P_{ICI} + \sigma_\varepsilon^2)}\right]\right\}. \tag{20}$$

For high SNR, i.e., when $\gamma \to \infty$, it can be seen that

$$\hat{C}_L^\infty = \frac{1}{N} E\left\{\sum_{k=0}^{N-1} \log_2\left[1 + \frac{\hat{H}_k \hat{H}_k^*}{(P_{ICI} + \sigma_\varepsilon^2)}\right]\right\}. \tag{21}$$

4. Block Markov Superposition Transmission in OFDM System

4.1. Encoding/decoding algorithm

At the transmitter, the incoming information bit sequence $\mathbf{u}$ is transformed into coded word $\mathbf{c}$, then the sequence $\mathbf{c}$ is mapped into a set of N-coded "frequency-domain" symbols $\mathbf{x} = [x_0, \cdots, x_{N-1}]^T$, in which the symbol x_i is equally likely chosen from a complex constellation $\mathcal{S}$ with $|\mathcal{S}| = 2^{M_c}$. In this section, we combine the BMST with an aforementioned $M_c N$-bit OFDM system under the fast fading channel. Let $\mathcal{C}[n, k]$ be a binary linear *basic code* of length n and dimension k. We assume that $n = M_c NB$ for some positive integer B. Let $\underline{\mathbf{u}}^{(t)} \in \mathbb{F}_2^k$ $(0 \le t \le L-1)$ be L sub-blocks of data to be transmitted. The encoding process with memory m is described in [16]. As for the decoding algorithm, we take the sliding-window decoding into account in the BMST-OFDM system. The reason is that the sliding-window decoding has a tunable delay and good performance, which are more suitable in the fast fading channel [17].

5. Numerical Results

In this section, we investigate the capacity bound and the BER performance in the OFDM system. All presented numerical examples are based on Monte Carlo simulation over fast fading channels according to the simulation parameters in Table 1. The wireless channels between the mobile antenna and the receiver antenna are modelled as Jakes' models [13]. The power delay profile (PDP) is exponential distribution with $\sigma_\ell^2 = \alpha e^{-0.6\ell}$, $0 \le \ell \le (L-1)$, where α is the normalization constant. For BMST encoding, uniform interleaves (randomly generated but fixed) are used, and the BMST encoder terminates every 100 data sub-blocks, i.e., $L = 100$. For decoding, the sliding-window algorithm is performed

with a maximum iteration number $J_{\max} = 18$ and an entropy stopping threshold $\delta_h = 10^{-5}$.

Table 1. Simulation parameters

Channel Bandwidth (B)	1.9MHz
Number of Subcarriers (N)	128
Subcarrier Spacing (F)	15kHz
Carrier Frequency (f_c)	2.0GHz
Number of Multipaths (L)	8
Cyclic Prefix Length (N_{cp})	9
Modulation Format	16QAM
Velocity	100-500km/h

Example 1. In this example, the capacity lower bound in the fast fading channel with perfect CSI is obtained according to the Equation (12). In Figure 2, it can be observed that the capacity decreases along with the increase of mobile velocity in fixed SNR, which is mainly due to the ICI power. It also indicates that the capacity lower bound changes very little with increasing velocity in the low SNR, but has a significant loss in the high SNR. In addition, when the mobile velocity is less than 200km/h, the capacity lower bound changes almost linearly as function of the average SNR. However, when the mobile velocity reaches 500km/h, the trend of the increase in the capacity is no longer linear due to the ICI power.

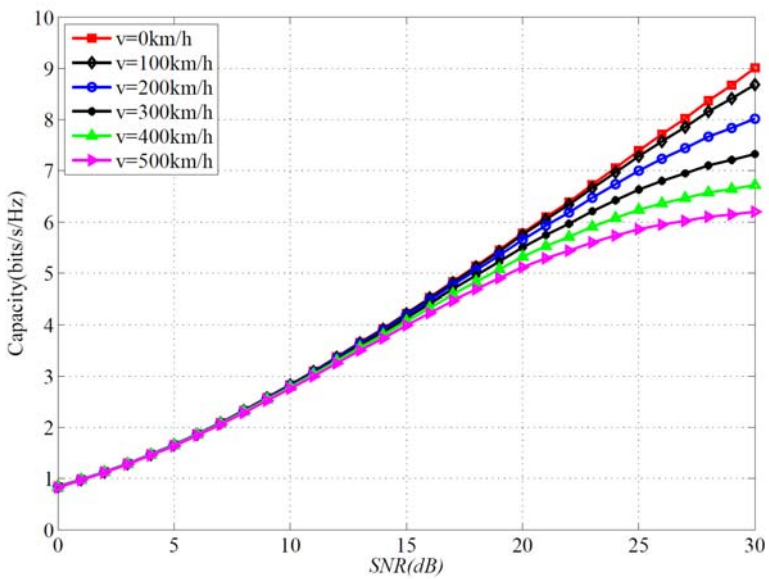

Figure 2. Capacity bound in the fast fading channel with perfect CSI for different velocity v = 0, 100, 200, 300, 400, 500km/h.

Example 2. The capacity lower bound of OFDM systems with imperfect CSI at speed 300km/h is shown in Figure 3, it shows that as the channel estimation becomes poor, the capacity bound decreases quickly. When the channel estimation error is $\sigma_e^2 = 0$, it indicates that the perfect CSI is performed. Similar trend can be observed in Figure 4. Furthermore, in Figure 4, we observe that the capacity bound gaps between $\sigma_e^2 = 0$ and $\sigma_e^2 = 1\%$ for velocity v = 0, 300, 500km/h are 3.33, 1.94, 0.97bit/s/Hz, respectively. This implies that the capacity loss for low speed systems are greater than for the high speed one in imperfect CSI, since the low speed systems are dependent on more accurate channel estimation to improve BER performance. In addition, it also shows that the capacity loss due to the channel estimation error is more greater than due to the ICI power. So we can conclude that the effect of channel estimation errors plays a critical role in the high mobile channel. Those results also show that the expressions of capacity bound for OFDM

systems with imperfect channel estimation is valid. On the other hand, as for different channel estimation error σ_e^2 = 0, 1.0%, 2.0%, 3.0%, 4.0%, 5.0%, the corresponding capacity limits achieving the spectral efficiency of 2 bits/s/Hz for 16QAM are 6.65, 6.81, 6.98, 7.13, 7.30dB, respectively.

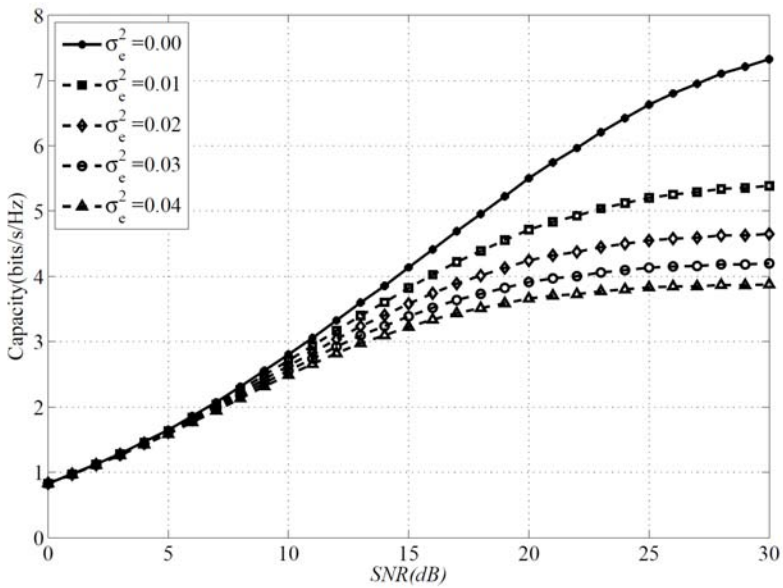

Figure 3. Ergodic capacity bound under fast fading channel with imperfect CSI for different channel estimation error, v = 300km/h.

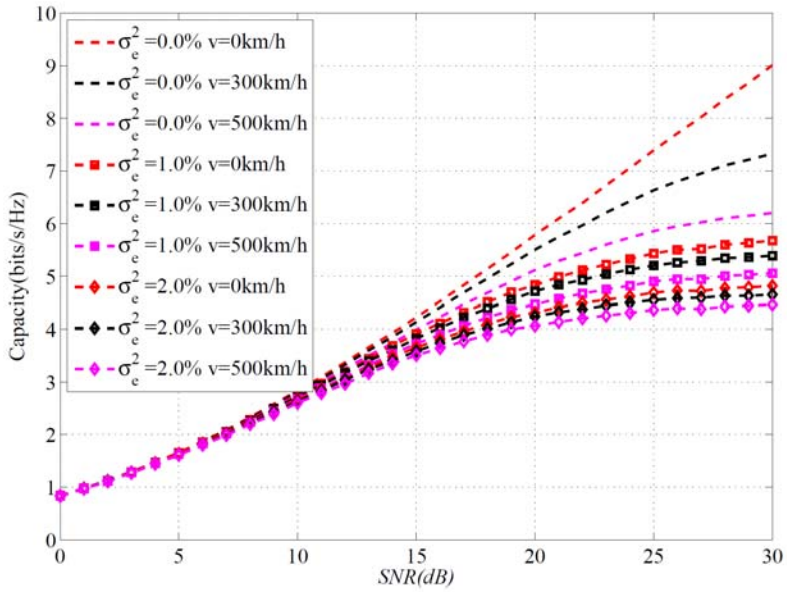

Figure 4. Ergodic capacity bound under fast fading channel with imperfect CSI for different channel estimation error, v = 0, 300, 500km/h.

Example 3. We construct a BMST-OFDM system with spectral efficiency of 2 bits/s/Hz with the Cartesian product of the single parity-check (SPC) code $[2, 1]^{6400}$ as the basic code. The BER performance results are shown in Figure 5 for the BMST-OFDM system with m = 2, 4 in the fast fading channel for v = 300km/h. As expected, along with the increase of the channel estimation error at the receiver, the BER performance is decreased. On the other hand, the BER performance with m = 4 becomes better the one with m = 2. The performance improvement is within 4.5dB at a BER 10^{-4}. On the other hand, it is seen that the gap of the BER performance curves for different channel estimation error is consistent with one of the capacity limits.

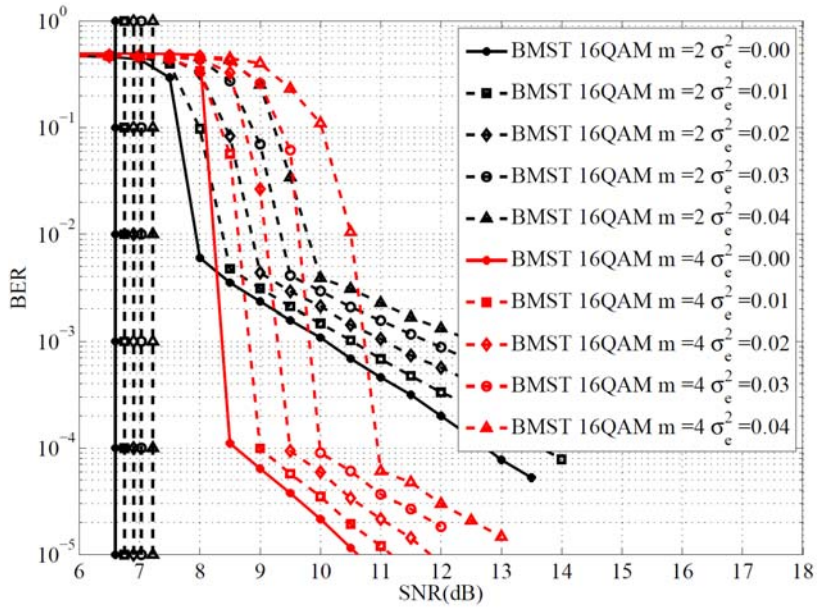

Figure 5. The BER performance of BMST under the fast fading channel for different channel estimation error, v = 300km/h, m = 2, 4,16QAM.

Example 4. We construct a BMST-OFDM system by spectral efficiency of 2 bits/symbol/carrier with the Cartesian product of the SPC code $[2, 1]^{3584}$ as the basic code. The memory and decoding latency are m = 4, d = 6, respectively. To make a fair comparison, a (3, 6) regular LDPC code is used in the OFDM system with the same code rate and decoding latency, in which codeword length of LDPC is 25088 bits. The simulation results are shown in Figure 6. It can be observed that, at the BER of 10^{-4}, the performance of BMST-OFDM has about 0.5dB gain compared with the LDPC-OFDM scheme. However, LDPC codes have a lower error floor.

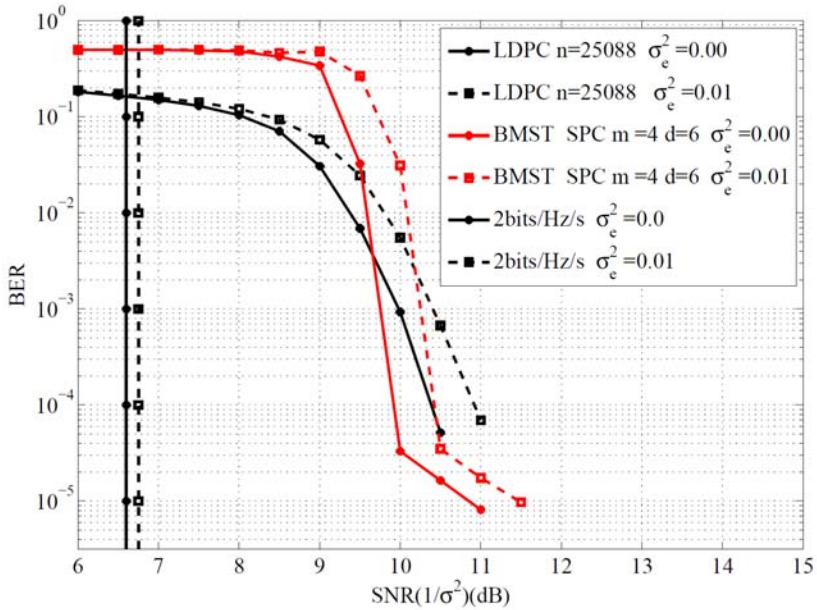

Figure 6. The BER performance of BMST-OFDM and LDPC-OFDM in the fast fading channel, v = 300km/h.

6. Conclusion

In this paper, based on the rapidly time-varying channel model in high-mobility environments, we derived expressions for the capacity lower bound of OFDM systems for the cases where the CSI are perfect and imperfect, respectively. We studied the influence of mobile velocity and channel state information on capacity lower bound. As a result, we can make a conclusion that the capacity lower bound decreases as the speed and channel estimation error increase, but the effect of channel estimation errors play a more critical role than the effect of ICI in the high mobile channel. In addition, we compare the performance of BMST-OFDM with LDPC-OFDM, the result shows that the performance of BMST-OFDM has about 0.5dB gain than LDPC-OFDM. However, LDPC codes have a lower error floor.

References

[1] M. Russell and G. L. Stuber, Interchannel interference analysis of OFDM in a mobile environment, in 1995 IEEE 45th Vehicular Technology Conference, IEEE 2 (1995), 820-824.

[2] J. C. Chuang, The effects of time delay spread on portable radio communications channels with digital modulation, IEEE Journal on Selected Areas in Communications 5(5) (1987), 879-889.

[3] J. Wang, H. Zhu and N. J. Gomes, Distributed antenna systems for mobile communications in high speed trains, IEEE Journal on Selected Areas in Communications 30(4) (2012), 675-683.

[4] E. Panayirci, H. Şenol and H. V. Poor, Joint channel estimation equalization and data detection for OFDM systems in the presence of very high mobility, IEEE Transactions on Signal Processing 58(8) (2010), 4225-4238.

[5] Y. Mostofi and D. C. Cox, ICI mitigation for pilot-aided ofdm mobile systems, IEEE Transactions on Wireless Communications 4(2) (2005), 765-774.

[6] S. -W. Hou and C. C. Ko, Intercarrier interference suppression for OFDM a uplink in time-and frequency-selective fading channels, IEEE Transactions on Vehicular Technology 58(6) (2009), 2741-2754.

[7] N. Sun and J. Wu, Maximizing spectral efficiency for high mobility systems with imperfect channel state information, IEEE Transactions on Wireless Communications 13(3) (2014), 1462-1470.

[8] L. Xiong, Z. Zhong, B. Ai and J. Qian, Ergodic and outage capacity for Ricean fading channel with shadow fading on high-speed railway, in 4th IET International Conference on Wireless, Mobile & Multimedia Networks (ICWMMN 2011) 2011.

[9] A. M. Tulino, G. Caire, S. Shamai and S. Verdú, Capacity of channels with frequency-selective and time-selective fading, IEEE Transactions on Information Theory 56(3) (2010), 1187-1215.

[10] H. Bölcskei, D. Gesbert and A. J. Paulraj, On the capacity of OFDM-based spatial multiplexing systems, IEEE Transactions on Communications 50(2) (2002), 225-234.

[11] M. Torabi, S. Aissa and M. R. Soleymani, systems with imperfect channel information: Capacity outage and BER performance, in IEEE International Conference on Communications 2006. ICC'06.12 IEEE (2006), 5342-5347.

[12] X. Ma, C. Liang, K. Huang and Q. Zhuang, Obtaining extra coding gain for short codes by block Markov superposition transmission, in IEEE International Symposium on Information Theory Proceedings (ISIT). IEEE (2013), 2054-2058.

[13] Y. R. Zheng and C. Xiao, Simulation models with correct statistical properties for Rayleigh fading channels, IEEE Transactions on Communications 51(6) (2003), 920-928.

[14] Z. Dong, P. Fan, E. Panayirci and P. T. Mathiopoulos, Effect of power and rate adaptation on the spectral efficiency of MQAM/OFDM system under very fast fading channels, EURASIP Journal on Wireless Communications and Networking 2012(1) (2012), 1-15.

[15] F. Hlawatsch and G. Matz, Wireless Communications Over Rapidly Time-Varying Channels, Elsevier, 2011.

[16] X. Ma, C. Liang, K. Huang and Q. Zhuang, Block Markov superposition transmission: Construction of big convolutional codes from short codes, IEEE Transactions on Information Theory 61(6) (2015), 3150-3163.

[17] X. Xu, C. Wang, Y. J. Zhu, X. Ma and X. Zhang, Block Markov superposition transmission of short codes for indoor visible light communications, IEEE Communications Letters 19(3) (2015), 359-362.

■